

000  
001  
002  
003  
004  
005  
006  
007  
008  
009  
010  
011  
012054  
055  
056  
057  
058  
059  
060  
061  
062  
063  
064  
065  
066  
067  
068  
069  
070  
071  
072  
073  
074  
075  
076  
077  
078  
079  
080  
081  
082  
083  
084  
085  
086  
087  
088  
089  
090  
091  
092  
093  
094  
095  
096  
097  
098  
099  
100  
101  
102  
103  
104  
105  
106  
107

## Supplemental Materials

Anonymous CVPR submission

Paper ID 481

### 1. Sample Data

We include some sample videos in our Multiview Action3D dataset in the supplemental materials, and the detection results of the proposed model.

The same action “pick up with one hand” taken from three different viewpoints. We can see that the spatio-temporal patterns of these three viewpoints differ significantly. This is a major challenge which we want to tackle in this paper. We showed that the proposed MST-AoG model can characterize the association of the spatio-temporal patterns across different viewpoints and achieve high accuracy and robustness for cross-view action recognition.

We have three experimental settings: cross-view setting uses training data and test data taken from different viewpoints; cross-subject setting uses training data and test data of different subjects; cross-environment setting uses training data and test data taken in different environments.

Our method not only classifies action but also parses action according to the And-Or graph using DP algorithm. For each frame, a parse graph is derived naturally representing the action category, pose and view angle in current frame. With the progress of the video, the parse graph may change and different nodes will be selected. We include some detection and parsing results of the proposed method in the demo video. The detection windows are obtained by using temporal median filters with frame 5 on the detection windows on all the frames. There are some failure parsing results due to big variation of appearance, but the classification of whole action is robust to those failures. Though currently we didn’t evaluate parsing performance quantitatively, we plan to evaluate it in the future.

### 2. Inference in AND/OR Graphs

The inference of a MST-AoG model calculates the states of the nodes and evaluates their scores to generate a parse graph, and uses the parse graph for action recognition. Since this MST-AoG model is tree-structured, we generate the parse graph using dynamic programming. The general dynamic programming process contains bottom-up phase and top-down phase, which is similar to sum-product and max-product algorithm in graphical model.

The bottom-up phase computes the node scores in a bottom-up manner. In the bottom-up phase, the score of an AND-node is computed according to the scores of its children:

$$s(n_{AND}, t_{n_{AND}}) = \max_{t_{n_1}, \dots, t_{n_l}} S_{n_{AND}}(s(n_1, t_{n_1}), \dots, s(n_l, t_{n_l}), t_{n_{AND}}) \quad (1)$$

where  $S_{n_{AND}}$  is the score function of the node  $n_{AND}$ ,  $t_{n_i}$  is the state of the node  $n_i$ .  $s(n_i, t_i)$  is the score of the state  $t_i$  of a node  $n_i$ , and  $n_1, \dots, n_l$  are the children of  $n_{AND}$ .

The score of an OR-node is the maximum scores of its children for the given state:

$$s(n_{OR}, t_{n_{OR}}) = \max_i S_{n_{OR}}(s(n_i, t_{n_i}), t_{n_{OR}}) \quad (2)$$

where  $S_{n_{OR}}$  is the score function of the node  $n_{OR}$ , and  $n_1, \dots, n_l$  are the children of  $n_{OR}$ .

We can compute the node scores bottom up from the leave nodes to the root node by iteratively applying Eq. (1) and Eq. (2).

The top-down phase computes the node states by passing the information back from the top root node down to the intermediate nodes. In the top-down phase, the state of a child of an AND-node can be updated as:

$$t_{n_i} = \arg \max_{t_{n_1}, \dots, t_{n_l}} S_{n_{AND}}(s(n_1, t_{n_1}), \dots, s(n_l, t_{n_l}), t_{n_{AND}}) \quad (3)$$

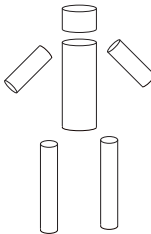


Figure 1. The configuration of the human parts.

Part	Joints
Head	head, left shoulder, right shoulder
Torso	left hip, right hip, spine, left shoulder, right
Left leg	left hip, left knee, left ankle, left foot
Right leg	right hip, right knee, right ankle, right foot
Left arm	left shoulder, left elbow, left wrist, left hand
Right arm	right shoulder, right elbow, right wrist, right hand

Table 1. The relationship between joints and parts.

and the state of a child of an OR-node can be updated as

$$t_{n_i} = \arg \max_{t_{n_i}} S_{n_{OR}}(s(n_i, t_{n_i}), t_{n_{OR}}) \quad (4)$$

In this way, we can compute the optimal state for the nodes in the AND-OR graph from the root node to the leave nodes by iteratively applying Eq. (3) and Eq. (4), and generate a parse graph.

### 3. The Human Part Configuration

In this paper, the human is represented as a set of human parts. Each human part consists of multiple human joints. We will describe the human part configuration in detail in this section.

The 3D joint positions are employed to characterize the pose of the human body. For a human subject, 20 joint positions are tracked by the skeleton tracker provided by Kinect. Each joint  $i$  has a 3-dimensional location coordinates vector  $\mathbf{p}_j(t) = (x_j(t), y_j(t), z_j(t))$ , a 3-dimensional motion vector  $\mathbf{m}_j(t) = (\Delta x_j(t), \Delta y_j(t), \Delta z_j(t))$  as well as a visibility label  $h_j(t)$  at a frame  $t$ .  $h_j(t) = 1$  denotes that the  $j$ -th joint is visible in frame  $t$  and  $h_j(t) = 0$  otherwise.

In this paper, we manually group the joints into the following six parts: head, torso, left arm, right arm, left leg and right leg. Each part is a cylinder that contains a set of tracked joints, illustrated in Fig. 1. The details of the part configuration are shown in Table 1.

In order to achieve invariance to absolute body position, the initial body orientation and the body size, we normalize the location and motion of the human joint. In the experiments we found the joints “head”, “neck”, “hip”, “left shoulder”, “right shoulder” to be the most stable. Thus, we use these joints to estimate an affine transformation matrix for each frame. This affine transformation matrix transforms the planes fitted by the 5 joints to the x-y plane and the joint “neck” to the origin. We can also obtain the azimuth rotation angle  $\theta(t)$  from the affine transformation matrix for each frame by factorizing the affine transformation matrix.

### 4. Samples of the Discriminative Poses

Some examples of the discriminative poses discovered with the proposed data mining algorithm is shown in Fig. 2. One subfigure in this figure corresponds to a discriminative pose for a specific action. We can see that one pose contains frames that are captured from different viewpoints and performed by different subjects. As a result, the frames for one pose can differ significantly in their appearance and motion. However, the proposed MST-AoG model can successfully represent the spatio-temporal patterns of one pose across different viewpoints.



Figure 2. Samples of the discovered discriminative poses. Each row shows a discriminative pose for one class, captured from different viewpoints. We can observe that one pose captured from different viewpoints have huge difference in the appearance and motion.

324

## 5. Representative and Discriminative Pose Mining Algorithm

378

325

The detail of the representative and discriminative pose mining algorithm is shown in Alg. 1. The definitions of the symbols in this algorithm can be found in the full paper.

379

326

380

327

381

328

382

329

383

1 Take a set of parts, and their candidate part items  $\mathcal{T}_k$ , the number of classes  $C$ , threshold  $T_{\text{supp}}$  and  $T_{\text{disc}}$ .

384

2 **for** Class  $c = 1$  to  $C$  **do**

385

3     Set  $P_c$ , the discriminative pose pool for class  $c$  to be empty :  $P_c = \{\}$ . Set  $k = 1$ .

386

4     **repeat**

387

5         1) Generate the candidates poses by augmenting the poses in the pool  $P_C$  with the part items of the  $k$ -th part  $\mathcal{T}_k$ .

388

6         2) Add the candidate poses whose support is larger than  $T_{\text{supp}}$  to the pool  $P_c$ .

389

7         3) Remove the poses in  $P_c$  that is non-maximal.

390

8         4)  $k = k + 1$

391

9     **until** no discriminative pose is added to  $P_c$ ;

392

10    remove the poses whose discriminative scores are less than  $T_{\text{disc}}$  in the pool  $P_c$ .

393

11 **end**

394

12 **return** the discriminative poses pool for all the classes.

395

**Algorithm 1:** Discriminative Pose Mining

342

396

343

397

344

398

345

399

346

400

347

401

348

402

349

403

350

404

351

405

352

406

353

407

354

408

355

409

356

410

357

411

358

412

359

413

360

414

361

415

362

416

363

417

364

418

365

419

366

420

367

421

368

422

369

423

370

424

371

425

372

426

373

427

374

428

375

429

376

430

377

431